J Shoulder Elbow Surg (2019) 28, 1146–1153

ELSEVIER

Journal of Shoulder and Elbow Surgery

www.elsevier.com/locate/ymse

The effect of glenohumeral radial mismatch on different augmented total shoulder arthroplasty glenoid designs: a finite element analysis

Vani J. Sabesan, MD[a,*], Diego J.L. Lima, MD[a], James D. Whaley, MD[b], Varun Pathak, MS[c], Liying Zhang, PhD[c]

[a]*Department of Orthopedic Surgery, Cleveland Clinic Florida, Weston, FL, USA*
[b]*Department of Orthopedic Surgery, Beaumont Health System, Royal Oak, MI, USA*
[c]*Department of Biomedical Engineering, Wayne State University School of Medicine, Detroit, MI, USA*

Background: Augmented glenoid implants to correct bone loss can possibly reconcile current prosthetic failures and improve long-term performance for total shoulder arthroplasty. Biomechanical implant studies have suggested benefits from augmented glenoid components, but limited evidence exists on optimal design.
Methods: An integrated kinematic finite element analysis (FEA) model was used to evaluate optimal augmented glenoid design based on biomechanical performance in translation in the anteroposterior plane similar to clinical loading and failure mechanisms with osteoarthritis. Computer-aided design software models of 2 different commercially available augmented glenoid designs—wedge (Equinox; Exactech, Inc., Gainesville, FL, USA) and step (STEPTECH; DePuy Synthes, Warsaw, IN, USA) were created according to precise manufacturer's dimensions of the implants. Using FEA, they were virtually implanted to correct 20° of retroversion. Two glenohumeral radial mismatches, 3.5/4 mm and 10 mm, were evaluated for joint stability and implant fixation simulating high-risk conditions for failure.
Results: The wedged and step designs showed similar glenohumeral joint stability under both radial mismatches. Surrogate for micromotion was a combination of distraction, translation, and compression. With similar behavior and measurements for distraction and translation, compression dictated micromotion (wedge: 3.5 mm = 0.18 mm and 10 mm = 0.10 mm; step: 3.5 mm = 0.19 mm and 10 mm = 0.25 mm). Stress levels on the backside of the implant and on the cement mantle were higher using a step design.
Discussion: Greater radial mismatch has the advantage of providing higher glenohumeral stability with tradeoffs, such as higher implant and cement mantle stress levels, and micromotion worse when using a step design.
Level of evidence: Basic Science Study; Computer Modeling

Keywords: Augmented glenoid; finite element analysis; step design; wedge design; total shoulder arthroplasty; glenoid bone loss; glenoid retroversion; radial mismatch

This study was exempt from Institutional Review Board approval because no animal or human subjects were studied.

*Reprint requests: Vani J. Sabesan, MD, Department of Orthopedics, Cleveland Clinic Florida, 2950 Cleveland Clinic Boulevard, Weston, FL 33331, USA.

E-mail address: sabesav@ccf.org (V.J. Sabesan).

Total shoulder arthroplasty (TSA) has proven to be successful in providing pain relief and restoring range of motion for patients with glenohumeral osteoarthritis. However, severe glenohumeral osteoarthritis frequently leads to glenoid retroversion and glenoid bone loss, which has been more

1058-2746/$ - see front matter
https://doi.org/10.1016/j.jse.2018.11.059

problematic with TSA.[7,12,22,23,25,26] Studies have shown that loosening of the implants is typically associated with the glenoid component (83% of cases) and is the most common reason for revision operations.[3,4,31] Under this circumstances, satisfactory implantation of the glenoid component is difficult to achieve and remains the most challenging aspect of TSA surgery.[1,9,11,16,18,21-23,25,32] Thus, the correction of glenoid retroversion and improved component positioning are major areas of interest in regards to optimizing outcomes for TSA.

Asymmetric "'high-side'" reaming of the anterior glenoid, glenoid bone grafting, or the use of an augmented glenoid component are the current options available to address posterior glenoid bone deficiency.[1,12-14,20,25,32] In cases with more severe glenoid retroversion, generally above 20°, asymmetric reaming may result in excessive bone removal such that a properly sized glenoid will perforate the glenoid wall and result in reduced stability.[17] The advantages of using wedge or step posterior augment glenoid designs are to better restore the native joint line, improve implant stability, decrease muscle shortening, and lessen bone removal to achieve full back side seating of the implant.[1,21,22,24]

Although the theoretical biomechanical rationale behind the augmented glenoid appears promising, limited evidence exists to support the augmented glenoid technology.[20] Finite element analysis (FEA) is a sophisticated form of biomechanical testing of shoulder prostheses used to provide detailed information regarding the loading behavior, localized stresses, and strains of the glenoid component. By analyzing relevant biomechanical parameters, FEA results have been shown to correlate with loosening mechanisms and predict reduced component stability with the standard components.[6,28-30]

The development of a finite element model of the shoulder examining the stresses and strains of the augmented glenoid will provide key insight into implant performance and optimal design. With rising medical costs, understanding the biomechanics of the augmented glenoid before clinical use would be beneficial if we can predict or identify factors contributing to failure or component loosening to minimize the occurrence of revision operations. The purpose of this study was to use an integrated kinematic FEA model to evaluate the optimal augmented glenoid design based on biomechanical performance with true muscle loading and translation in the anterior-posterior (AP) plane most similar to real time clinical loading and failure mechanisms for TSA.

Materials and methods

This biomechanical study tested 2 different commercially available augmented glenoid implant designs (wedge and step) comparing different glenohumeral conformity settings to evaluate the effects on mechanical parameters related to loosening and fixation failure. The 2 settings of radial mismatch modeled were based on optimal (3.5 mm [wedge]/4 mm [step]) and high-risk conditions (10 mm [wedge and step]) to identifying failure mechanisms based on the literature. The mismatch conditions were obtained by reducing the humeral head diameters.

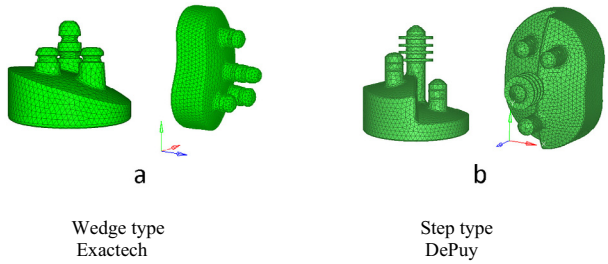

Figure 1 Finite element models of the augmented (**a**) wedge and (**b**) step glenoid component designs. Exatech Inc., Gainesville, FL, USA; DePuy Synthes, Warsaw, IN, USA.

Glenoid component and model generation

The 2 augmented glenoid component designs modeled were an all-polyethylene peg curved back step design (Global STEPTECH; DePuy Synthes, Inc., Warsaw, IN, USA) and an all-polyethylene wedge glenoid design (Equinoxe; Exactech, Inc., Gainesville, FL, USA). All components were constructed as computer-aided design (CAD) models, and the geometry of the implant components was used to develop finite element models with 1-mm element resolution using HyperMesh (Altair Engineering, Inc., Troy, MI, USA), ICEM-CFD (ANSYS Inc., Canonsburg, PA, USA), and ANSA (BETA CAE Systems, Root, Switzerland) based on CAD data processed with MIMICS (Materialise, Leuven, Belgium). The FEA simulations were performed using a commercial nonlinear explicit FEA software LS-Dyna (LSTC, Livermore, CA, USA; Fig. 1).

The material of the glenoid implant was modeled as linearly elastic, isotropic, homogeneous material of high molecular weight. The polymethyl methacrylate bone cement material was defined with Young's modulus of 2.0 GPa and Poisson's ratio of 0.23. A rigid humeral head model was used based on manufacturer design defined as rigid cobalt chromium alloy (Table I). The glenoid bone model was considered as a linear elastic material with nonhomogeneous properties related to its density simulating both cortical and cancellous properties.[19]

Finite element model setup for ASTM simulation testing

A standard ASTM test that evaluates glenoid loosening or dissociation (F2028-08) from humeral head translation in an AP direction was used to validate our model. To investigate the mechanical effect of different augmented implant designs on the scapula bone, FEA models of the scapula bone were developed and integrated with the validated glenoid models described above (Fig. 2, *a*). The geometry of the scapula of the shoulder was taken from the Global Human Body Models Consortium (GHBMC, Troy, MI, USA) 50th percentile male human body model developed and validated.[24] This scapula model was based on CAD data obtained from the computed tomography and magnetic resonance imaging scans of a 50th percentile male subject. The mesh of the scapula bone was removed to simulate a 20° retroverted shoulder, and the appropriate augmented implant designs were fitted to the respective scapula model to simulate desired retroversion correction (+7 mm for the step style design and 16° for the wedge style design).

Table I Material properties defined for the finite element wedge and the step model

Component name	Material model	Property	
Wedge model			
Humeral head implant	Elastic model	Rho (kg/mm^3)	7.90E-06
		E (GPa)	210
		Nu	0.3
Glenoid implant (polyethylene)	Piecewise elastic	Rho (kg/mm^3)	1.00E-06
		E (GPa)	1.26
		Nu	0.46
		Yield strength (GPa)	0.021
Cement (PMMA)	Piecewise elastic	Rho (kg/mm^3)	1.00E-06
		E (GPa)	2
		Nu	0.23
Mounting block (polyurethane)	Foam model	Rho (kg/mm^3)	3.20E-07
		E (GPa)	0.193
Step model			
Humeral head implant	Elastic model	Rho (kg/mm^3)	7.90E-06
		E (GPa)	210
		Nu	0.3
Glenoid implant (polyethylene)	Piecewise elastic	Rho (kg/mm^3)	1.00E-06
		E (GPa)	0.52
		Nu	0.46
		Tangential modulus (GPa)	0.1
		Yield strength (GPa)	0.012
Cement (PMMA)	Piecewise elastic	Rho (kg/mm^3)	1.00E-06
		E (GPa)	2
		Nu	0.23
Mounting block (polyurethane)	Foam model	Rho (kg/mm^3)	3.20E-07
		E (GPa)	0.193

PMMA, polymethyl methacrylate; *Rho*, defines the density of the material; *kg/mm^3*, kilograms per 1 cubic millimeter; *E* is the Young's modules that defines material's stiffness; *GP*, gigapascals; *Nu*, defines Poisson's ration.

The cement elements were generated between the bone and implant at the proper site according to the manufacturer's specification. The implant–cement–bone interfaces were bonded directly via nodal connectivity (Fig. 3). Cement was placed over the pegs of the implant based on the manufacturer's instruction specified for the type of glenoid models. The cement was directly connected to the polyurethane block and the implant peg (Fig. 2, *b*).

Finite element model simulation

An axial load of 750 N was applied perpendicular to the glenoid implant, and the humeral head translation occurred along the true AP axis of the glenoid with 25 mm/s shear movement applied in the parallel direction of glenoid by the humeral head to recreate edge loading.[23] The rest of the direction was constrained and no rotation was allowed (Fig. 4).

The AP translation of the humeral head was simulated based on the loading used in the ASTM test to investigate the biomechanical responses of the bone and compare the 2 different augment designs. Each implant underwent 50,000 cycles at constant frequency of 2 Hz. This cyclic loading represents approximately 25 high-load activities per day (ie, getting out of a chair or lifting a suitcase) for 5 years.[23]

The glenohumeral subluxation force, glenoid micromotion (compression, distraction, and translation), and shear stress levels were calculated by the FEA models and compared between the 2 designs to evaluate the effect of the glenohumeral conformity. Validation of the FEA models at 3.5 mm and 10 mm radial mismatch for wedge design and 4 and 10 mm for step designs was achieved through direct comparison with the results from the ASTM tests by Anglin et al[2] and Sabesan et al,[23] respectively, to ensure the accuracy of the mechanical responses as predicted by the FEA models.

Outcome variables

The outcome variables were model-predicted biomechanical responses, including glenohumeral contact force, backside of the implant, and cement mantle stresses, as well as micromotion at the bone–cement interface between the 2 augmented designs.

Results

Force ratio

The shear force required to assess instability was expressed as a ratio of shear force compared with the applied compressive force, defined as the force ratio.[10] The step model had a slightly higher force ratio than the wedge design at similar conformity settings (Table II). The results showed that the force ratio increased as the radial mismatch increased for both glenoid designs.

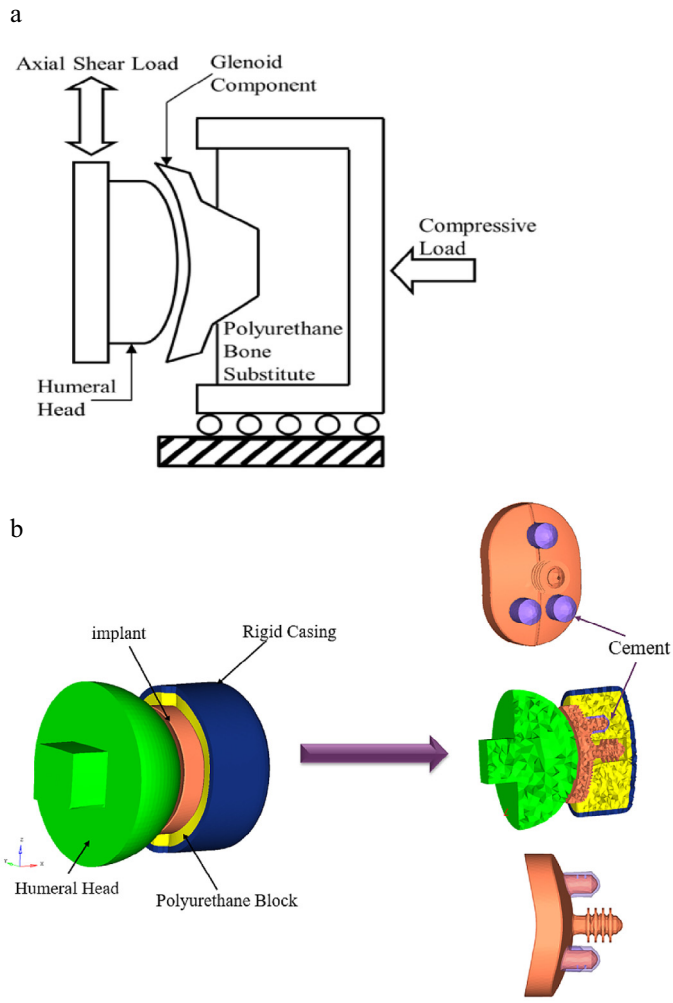

Figure 2 (**a**) Schematic ASTM subluxation test, and (**b**) finite element model setup for ASTM subluxation test simulation: The contact interface was defined between the back of the glenoid implant and the bone substitute.

Table II Shearing force required to instigate humeral instability

Implant design	Radial mismatch*	Force ratio
Wedge†	3.5	0.69
	10	0.70
Step‡	4	0.72
	10	0.75

* Radial mismatch between the humeral head and glenoid prosthetic components, in mm.
† 18° backside full wedge.
‡ 7 mm backside step.

Micromotion

Micromotion was defined as a combination of 3 components based on different axes directions (Fig. 5). At optimal radial mismatch (3.5/4 mm), the wedge design showed higher overall micromotion. The distraction and compression measurements were similar between implants, at 0.042 mm for the wedge and 0.040 mm for the step design and at 0.18 mm for the wedge and 0.19 mm for the step design, respectively. Translation measurements were higher for the wedge design (0.058 mm) than for the step design (0.023 mm) at lower radial mismatch settings. With a higher mismatch ratio, the step design registered higher micromotion at extreme conditions

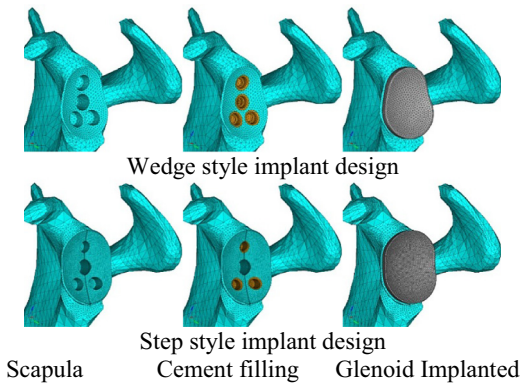

Figure 3 Finite element models of the scapula, cement, and implanted glenoid for 2 implant designs.

Table III Measurements of compression during finite element model biomechanical testing

Implant design	Radial mismatch*	Compression†
Wedge‡	3.5	0.18
	10	0.10
Step§	4	0.19
	10	0.25

* Radial mismatch between the humeral head and glenoid prosthetic components, in mm.
† Micromotion towards the bone substitute, within the x axis, in mm.
‡ 18° backside full wedge.
§ 7 mm backside step.

Table IV Measurements of distraction during FE model biomechanical testing

Implant design	Radial mismatch*	Distraction†
Wedge‡	3.5	0.042
	10	0.030
Step§	4	0.040
	10	0.027

* Radial mismatch between the humeral head and glenoid prosthetic components, in mm.
† Micromotion away from the bone substitute, within the *x* axis, in mm.
‡ 18° backside full wedge.
§ 7 mm backside step.

(Table III) which was driven primarily by compression. Again, the wedge and step designs had similar results for distraction and translation at high-risk conditions of radial mismatch (Tables IV and V), but there were significant differences in compression (wedge: 0.10 mm; step: 0.25 mm).

Glenoid component shear stress levels

Concerning implant shear stress, the results measured on the backside of the component were 12.5 MPa (3.5-mm mismatch) and 17.6 MPa at 10 mm of radial mismatch for the wedge design and 13.4 MPa for 4 mm and 18.6 MPa at 10 mm of radial mismatch for the step design (Table VI).

Table V Measurements of translation during FE model biomechanical testing

Implant design	Radial mismatch*	Translation†
Wedge‡	3.5	0.058
	10	0.062
Step§	4	0.023
	10	0.063

* Radial mismatch between the humeral head and glenoid prosthetic components, in mm.
† Micromotion within the superior-inferior axis parallel to the glenoid plane, in mm.
‡ 18° backside full wedge.
§ 7 mm backside step.

Table VI Measurements of backside implant peak shear stress during finite element model biomechanical testing

Implant design	Radial mismatch*	Backside stress†
Wedge‡	3.5	12.5
	10	17.6
Step§	4	13.4
	10	18.6

* Radial mismatch between the humeral head and glenoid prosthetic components, in mm.
† Backside implant peak shear stress, in MPa.
‡ 18° backside full wedge.
§ 7 mm backside step.

Cement shear stress levels

The cement shear stress levels observed were 2.9 MPa at 3.5 mm and 2.6 MPa at 10 mm of radial mismatch for the wedge design compared with 4.4 MPa at 3.5 mm and 4.1 MPa at 10 mm of radial mismatch for the step design (Table VII). The step model showed the highest stress levels under different conditions and measured at different locations.

Discussion

Posterior glenoid wear is a common consequence of glenohumeral osteoarthritis and a significant factor affecting outcomes for glenoid component in TSA.[1,8,15] Placement of the glenoid in excessive retroversion leads to eccentric loading, subluxation of the humeral head, and early loosening.[1,3,6,7,10,12,18,25] Studies have demonstrated asymmetric reaming for correction of glenoid retroversion over 20° results in medialization of the joint line due to excessive bone removal and peg perforation.[21] One solution proposed is the use of an all-polyethylene augmented glenoid component to manage moderate to severe glenoid bone loss. Our aim was to use a integrated kinematic FEA of a TSA to evaluate which augmented glenoid design (wedge vs. step) would be optimal to reduce excessive stresses on the implant and cement mantle and minimize micromotion.

Table VII Measurements of cement mantle peak shear stress during finite element model biomechanical testing

Implant design	Radial mismatch*	Cement stress†
Wedge‡	3.5	2.9
	10	2.6
Step§	4	4.4
	10	4.1

* Radial mismatch between the humeral head and glenoid prosthetic components, in mm.
† Cement mantle peak shear stress, in MPa.
‡ 18° backside full wedge.
§ 7 mm backside step.

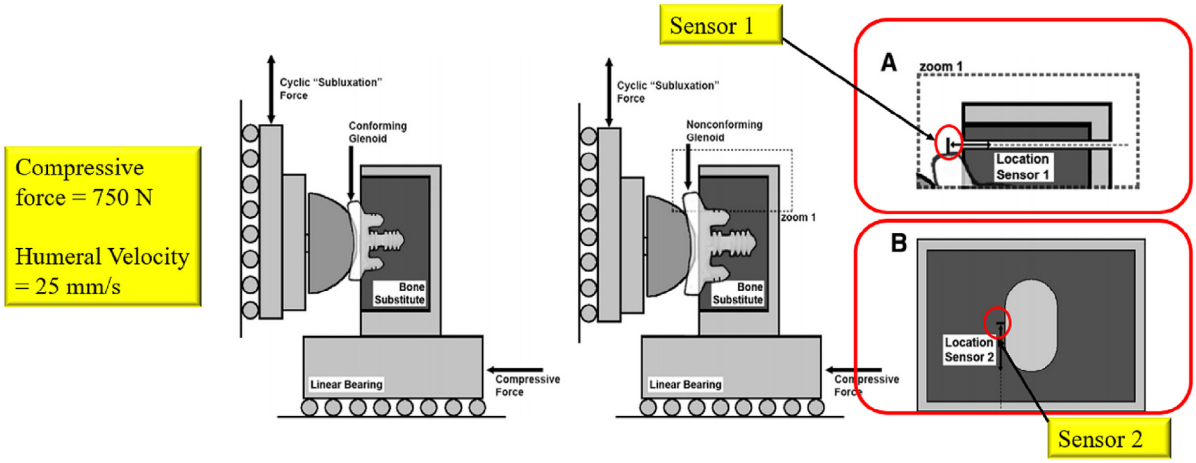

Figure 4 This figure depicts the location of sensors to predict the mechanical response of implant and bone during superior-inferior and anterior-posterior direction for finite element simulation. (**A**) One differential variable reluctant transducer sensor was fitted at the superior pole of the glenoid, as recommended by ASTM standards, to measure glenoid distraction and compression. (**B**) The second sensor was fitted at the lateral side of the glenoid parallel to the axis of actuator motion for the measurement of inferior-superior glenoid translation.

Our results suggest that the wedge glenoid design may have a better performance and fixation profile under different radial mismatch settings; however, further clinical research is needed to verify these biomechanical results.[2] Our results for implant fixation demonstrated that differences in augmented glenoid designs based on the amount of micromotion were predominantly driven by compression, with the step design demonstrating higher amounts of micromotion and risk of implant loosening.

These differences in micromotion comparing step vs. wedge designs differed from previously reported literature.[19,23,24] Iannotti et al[10] studied the effect of implant design at liftoff as a surrogate for micromotion and implant fixation in foam block models. Their results may have differed from ours due

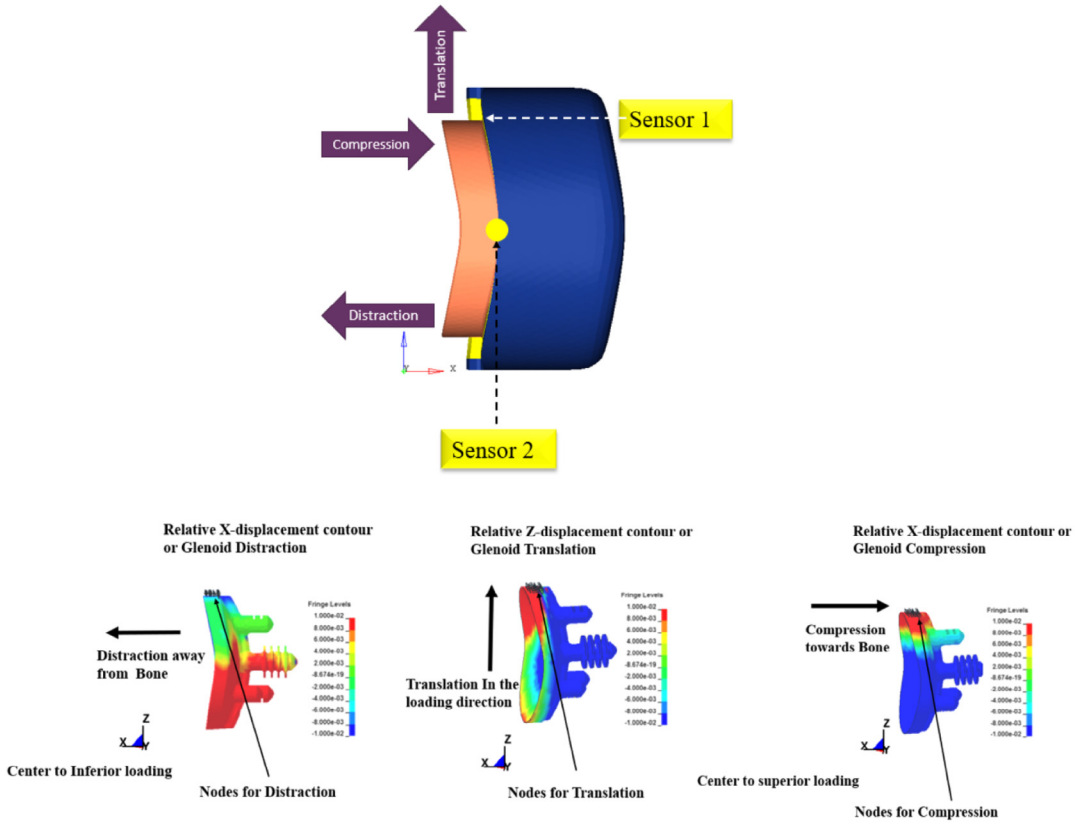

Figure 5 Micromotion resolved into 3 movements—distraction, translation, and compression—relative to the fixed scapular bone substitute.

to differences in methodology because we were able to simulated muscle loading and bone fixation in a validated kinematic FEA model compared with their foam block model. In addition, we did not specifically examine liftoff and looked at 2 variations in mismatch to truly characterize humeral subluxation or eccentric loading.[10]

It appears not only loading conditions but also design variations are important considerations when examining implant fixation and micromotion. Because Wahab et al[24] suggested that using an additional fifth peg will result in superior fixation stability to resist off center loading compared to the two 4-peg designs, we examined in our results. Further studies on micromotion must combine loading conditions and critical implant design features to better understand fixation and micromotion for augmented glenoid components.

Studies have found significantly larger interface micromotion when the radial mismatch between the humeral head and the glenoid exceeded 6 mm.[23,27] However, previous studies examined a cementless glenoid component with a metal-backed, round, posteriorly curved implant with a central screw mounted in a rigid polyurethane bone substitute. Whereas the optimal glenohumeral mismatch in cemented pegged glenoid implants is multifactorial and has not been fully defined, our results support data from previous studies that there are increased stress levels with increased glenohumeral radial mismatch greater than 10 mm and the subsequent risk of increasing glenoid micromotion and loosening.[23] These higher stress levels and micromotion contrast previous studies showing a correlation between of glenohumeral prosthetic radial mismatch and glenoid radiolucent lines.[11,34]

Walch et al[33] analyzed the postoperative radiographs of 319 patients who underwent primary TSA with prostheses that exhibited different degrees of glenohumeral radial mismatch (<4 mm, 4.5-5.5 mm, 6-7 mm, and 7-10 mm) and found a lower extent of radiolucency was significantly associated with radial mismatches in excess of 5.5 mm. They concluded that radial mismatch was significantly associated with glenoid radiolucent lines that were least when the radial mismatch was between 6 and 10 mm.[33]

Although there was a tradeoff for better joint stability, the level of stress on the backside of the implant and in the cement mantle were both higher at both radial mismatch settings using a step design. In addition, our results showed that the cement mantle endurance limit of 4 MPa was exceeded for the step design, suggesting concerns for initial implant fixation with the step design.[32] There is concern with increased initial cement mantle stresses contributing to increase risk of failure or fracture of the cement mantle. The literature shows that component loosening has been reported to occur at the bone–cement interface, within the cement mantle itself, or at the component–cement interface.[15]

The development of an accurate kinematic combined finite element model of the total shoulder, inclusive of all relevant muscle structures, geometry, and nonhomogeneity of the glenoid, remains challenging.[8] Notwithstanding, it has been used in several studies of the glenohumeral joint during the past decade, which is an indication of its current value and future potential. One of the advantages of a finite element model is that it can be used to virtually determine biomechanical responses such as displacement and stress.[5] Finite element models may provide information on dislocation load, humeral head translation, joint contact pressures, material deformation, and fixation stresses that are difficult, if not impossible, to obtain using laboratory tests.

Some limitations should be considered for this study. An average 50th percentile man was used as our joint model, which can only be extrapolated to all patients to a certain extent. Our analysis simulated at least 5 years of implant wear under minimal loading conditions and without range of motion of the studied joint. In a real-life situation, our prosthetic joint would be under the influence of multidirectional loading conditions that may affect our results.

Conclusion

Posterior glenoid wear is a common consequence of glenohumeral osteoarthritis and a significant factor affecting outcomes for the glenoid component in total shoulder arthroplasty. One solution proposed is the use of all-polyethylene augmented glenoid component to manage moderate to severe glenoid bone loss. Our results suggest that the wedge glenoid design may have a better performance and fixation profile under different radial mismatch settings; however, further clinical research is needed to verify these biomechanical results. Our FEA model shows that increasing radial mismatch generated disadvantages for both implants. Nonetheless, the wedge design presented with lower overall micromotion and stress levels on the implant and cement mantle. We can expect a wedged glenoid implant design to have lower risks of implant loosening and failure or fracture over time, which may lead to better clinical outcomes and lower revision rates.

Disclaimer

This work received Orthopaedic Research and Education Foundation grants.

Vani J. Sabesan is a paid consultant for Arthrex Inc. and receives research support from Exactech Inc. The other authors, their immediate families, and any research foundations with which they are affiliated have not received any financial payments or other benefits from any commercial entity related to the subject of this article.

References

1. Allred JJ, Flores-Hernandez C, Hoenecke HR Jr, D'Lima DD. Posterior augmented glenoid implants require less bone removal and generate lower stresses: a finite element analysis. J Shoulder Elbow Surg 2016;25:823-30. http://dx.doi.org/10.1016/j.jse.2015.10.003

2. Anglin C, Wyss UP, Pichora DR. Mechanical testing of shoulder prostheses and recommendations for glenoid design. J Shoulder Elbow Surg 2000;9:323-31.
3. Cheung EV, Sperling JW, Cofield RH. Revision shoulder arthroplasty for glenoid component loosening. J Shoulder Elbow Surg 2008;17:371-5. http://dx.doi.org/10.1016/j.jse.2007.09.003
4. Cil A, Veillette CJ, Sanchez-Sotelo J, Sperling JW, Schleck CD, Cofield RH. Survivorship of the humeral component in shoulder arthroplasty. J Shoulder Elbow Surg 2010;19:143-50. http://dx.doi.org/10.1016/j.jse.2009.04.011
5. Denard PJ, Lederman E, Parsons BO, Romeo AA. Finite element analysis of glenoid-sided lateralization in reverse shoulder arthroplasty. J Orthop Res 2017;35:1548-55. http://dx.doi.org/10.1002/jor.23394
6. Farron A, Terrier A, Büchler P. Risks of loosening of a prosthetic glenoid implanted in retroversion. J Shoulder Elbow Surg 2006;5:521-6. http://dx.doi.org/10.1016/j.jse.2005.10.003
7. Hermida JC, Flores-Hernandez C, Hoenecke HR, D'Lima DD. Augmented wedge-shaped glenoid component for the correction of glenoid retroversion: a finite element analysis. J Shoulder Elbow Surg 2014;23:347-54. http://dx.doi.org/10.1016/j.jse.2013.06.008
8. Hopkins AR, Hansen UN, Amis AA. Finite element models of total shoulder replacement: Application of boundary conditions. Comput Methods Biomech Biomed Engin 2005;8:39-44. http://dx.doi.org/10.1080/10255840500075205
9. Hopkins AR, Hansen UN, Amis AA, Emery R. The effects of glenoid component alignment variations on cement mantle stresses in total shoulder arthroplasty. J Shoulder Elbow Surg 2004;13:668-75. http://dx.doi.org/10.1016/j.jse.2004.04.008
10. Hopkins AR, Hansen UN, Amis AA, Taylor M, Emery RJ. Glenohumeral kinematics following total shoulder arthroplasty: a finite element investigation. J Orthop Res 2007;25:108-15. http://dx.doi.org/10.1002/jor.20290
11. Hopkins AR, Hansen UN, Amis AA, Taylor M, Gronau N, Anglin C. Finite element modelling of glenohumeral kinematics following total shoulder arthroplasty. J Biomech 2006;39:2476-83. http://dx.doi.org/10.1016/j.jbiomech.2005.07.031
12. Iannotti JP, Lappin KE, Klotz CL, Reber EW, Swope SW. Liftoff resistance of augmented glenoid components during cyclic fatigue loading in the posterior-superior direction. J Shoulder Elbow Surg 2013;22:1530-6. http://dx.doi.org/10.1016/j.jse.2013.01.018
13. Knowles NK, Ferreira LM, Athwal GS. Augmented glenoid component designs for type B2 erosions: A computational comparison by volume of bone removal and quality of remaining bone. J Shoulder Elbow Surg 2015;24:1218-26. http://dx.doi.org/10.1016/j.jse.2014.12.018
14. Knowles NK, Keener JD, Ferreira LM, Athwal GS. Quantification of the position, orientation, and surface area of bone loss in type B2 glenoids. J Shoulder Elbow Surg 2015;24:503-10. http://dx.doi.org/10.1016/j.jse.2014.08.021
15. Lewis GS, Brenza JB, Paul EM, Armstrong AD. Construct damage and loosening around glenoid implants: a longitudinal micro-CT study of five cadaver specimens. J Orthop Res 2016;34:1053-60. http://dx.doi.org/10.1002/jor.23119
16. Mansat P, Briot J, Mansat M, Swider P. Evaluation of the glenoid implant survival using a biomechanical finite element analysis: influence of the implant design, bone properties, and loading location. J Shoulder Elbow Surg 2007;16(Suppl.):S79-83. http://dx.doi.org/10.1016/j.jse.2005.11.010
17. Nowak DD, Bahu MJ, Gardner TR, Dyrszka MD, Levine WN, Bigliani LU, et al. Simulation of surgical glenoid resurfacing using three-dimensional computed tomography of the arthritic glenohumeral joint: the amount of glenoid retroversion that can be corrected. J Shoulder Elbow Surg 2009;18:680-8. http://dx.doi.org/10.1016/j.jse.2009.03.019
18. Nyffeler RW, Sheikh R, Atkinson TS, Jacob HA, Favre P, Gerber C. Effects of glenoid component version on humeral head displacement and joint reaction forces: an experimental study. J Shoulder Elbow Surg 2006;15:625-9. http://dx.doi.org/10.1016/j.jse.2005.09.016
19. Rice JC, Cowin SC, Bowman JA. On the dependence of the elasticity and strength of cancellous bone on apparent density. J Biomech 1988;21:155-68.
20. Rice RS, Sperling JW, Miletti J, Schleck C, Cofield RH. Augmented glenoid component for bone deficiency in shoulder arthroplasty. Clin Orthop Relat Res 2008;466:579-83. http://dx.doi.org/10.1007/s11999-007-0104-4
21. Roche CP, Diep P, Grey SG, Flurin PH. Biomechanical impact of posterior glenoid wear on anatomic total shoulder arthroplasty. Bull Hosp Jt Dis 2013;(Suppl. 2):S5-11. https://www.ncbi.nlm.nih.gov/pubmed/24328573
22. Sabesan V, Callanan M, Sharma V, Iannotti JP. Correction of acquired glenoid bone loss in osteoarthritis with a standard versus an augmented glenoid component. J Shoulder Elbow Surg 2014;23:964-73. http://dx.doi.org/10.1016/j.jse.2013.09.019
23. Sabesan VJ, Ackerman J, Sharma V, Baker KC, Kurdziel MD, Wiater JM. Glenohumeral mismatch affects micromotion of cemented glenoid components in total shoulder arthroplasty. J Shoulder Elbow Surg 2015;24:814-22. http://dx.doi.org/10.1016/j.jse.2014.10.004
24. Schwartz D, Guleyupoglu B, Koya B, Stitzel JD, Gayzik FS. Development of a computationally efficient full human body finite element model. Traffic Inj Prev 2015;16:49-56. http://dx.doi.org/10.1080/15389588.2015.1021418
25. Shapiro TA, McGarry MH, Gupta R, Lee YS, Lee TQ. Biomechanical effects of glenoid retroversion in total shoulder arthroplasty. J Shoulder Elbow Surg 2007;16(Suppl.):90-5. http://dx.doi.org/10.1016/j.jse.2006.07.010
26. Streit JJ, Shishani Y, Greene ME, Nebergall AK, Wanner JP, Bragdon CR, et al. Radiostereometric and radiographic analysis of glenoid component motion after total shoulder arthroplasty. Orthopedics 2015;38:e891-7. http://dx.doi.org/10.3928/01477447-20151002-56
27. Suárez DR, Nerkens W, Valstar ER, Rozing PM, van Keulen F. Interface micromotions increase with less-conforming cementless glenoid components. J Shoulder Elbow Surg 2012;21:474-82. http://dx.doi.org/10.1016/j.jse.2011.03.008
28. Terrier A, Brighenti V, Pioletti DP, Farron A. Importance of polyethylene thickness in total shoulder arthroplasty: a finite element analysis. Clin Biomech (Bristol, Avon) 2012;http://dx.doi.org/10.1016/j.clinbiomech.2011.12.003
29. Terrier A, Büchler P, Farron A. Influence of glenohumeral conformity on glenoid stresses after total shoulder arthroplasty. J Shoulder Elbow Surg 2006;15:515-20. http://dx.doi.org/10.1016/j.jse.2005.09.021
30. Terrier A, Büchler P, Farron A. Bone-cement interface of the glenoid component: stress analysis for varying cement thickness. Clin Biomech (Bristol, Avon) 2005;20:710-7. http://dx.doi.org/10.1016/j.clinbiomech.2005.03.010
31. Wirth MA, Rockwood CA Jr. Complications of total shoulder-replacement arthroplasty. J Bone Joint Surg Am 1996;78:603-16
32. Yongpravat C, Kim HM, Gardner TR, Bigliani LU, Levine WN, Ahmad CS. Glenoid implant orientation and cement failure in total shoulder arthroplasty: a finite element analysis. J Shoulder Elbow Surg 2013;22:940-7. http://dx.doi.org/10.1016/j.jse.2012.09.007
33. Zhang J, Yongpravat C, Kim HM, Levine WN, Bigliani LU, Gardner TR, et al. Glenoid articular conformity affects stress distributions in total shoulder arthroplasty. J Shoulder Elbow Surg 2013;22:350-6. http://dx.doi.org/10.1016/j.jse.2012.08.025
34. Zumstein V, Kraljevic M, Hoechel S, Conzen A, Nowakowski AM, Muller-Gerbl M. The glenohumeral joint—a mismatching system? A morphological analysis of the cartilaginous and osseous curvature of the humeral head and the glenoid cavity. J Orthop Surg Res 2014;9:34. http://dx.doi.org/10.1186/1749-799X-9-34